

## Shell Model Monte Carlo Studies of $\gamma$ -Soft Nuclei

Y. Alhassid,<sup>1</sup> G. F. Bertsch,<sup>2</sup> D. J. Dean,<sup>3,4</sup> and S. E. Koonin<sup>3</sup>

<sup>1</sup>Center for Theoretical Physics, Sloane Physics Laboratory, Yale University, New Haven, Connecticut 06520

<sup>2</sup>Department of Physics and Institute for Nuclear Theory, University of Washington, Seattle, Washington 98195

<sup>3</sup>W. K. Kellogg Radiation Laboratory, 106-38, California Institute of Technology, Pasadena, California 91125

<sup>4</sup>Physics Division, Oak Ridge National Laboratory, Oak Ridge, Tennessee 37831

(Received 10 August 1995)

We present shell model Monte Carlo calculations for nuclei in the full major shell 50–82 for both protons and neutrons. For the interaction we use a pairing plus quadrupole derived from a surface-peaked separable force. The methods are illustrated for  $^{124}\text{Sn}$ ,  $^{128}\text{Te}$ , and  $^{124}\text{Xe}$ . We calculate shape distributions, moments of inertia, and pairing correlations as functions of temperature and angular velocity. Our calculations are the first microscopic evidence of  $\gamma$ -softness of nuclei in this region. [S0031-9007(96)00894-0]

PACS numbers: 21.60.Ka, 21.10.Gv, 21.60.Cs, 27.60.+j

Nuclei with mass number  $100 \leq A \leq 140$  are believed to have large shape fluctuations in their ground states. Associated with this softness are spectra with an approximate O(5) symmetry and bands with energy spacings intermediate between rotational and vibrational. The geometrical model describes these nuclei by potential energy surfaces with a minimum at  $\beta \neq 0$ , but independent of  $\gamma$  [1]. Some of these nuclei have been described in terms of a quartic five-dimensional oscillator [2]. In the interacting boson model (IBM), they are described by an O(6) dynamical symmetry [3].

Nuclei with  $100 \leq A \leq 140$  fill the major shell between 50 and 82 for both protons and neutrons, and conventional shell model calculations in the full space are impossible for many of these nuclei. However, with the introduction of shell model Monte Carlo techniques (SMMC) [4], it has become possible to do exact calculations (up to a statistical error) in much larger model spaces [5] at zero and finite temperatures. This Letter presents the first fully microscopic calculations for soft nuclei with  $100 \leq A \leq 140$  and compares them with the results of more phenomenological models.

An important problem is the choice of the interaction. It was recently shown that the realistic residual nuclear force is dominated by a pairing plus quadrupole interaction [6]. We have used such an interaction, where the pairing contains both monopole and quadrupole [7] terms whose strengths are determined by odd-even mass differences. The quadrupole interaction is derived from a surface-peaked separable force [8]. Such an interaction is expected to be a reasonable way of describing deformation and pairing phenomena. A major advantage of this interaction is that it has a “good” Monte Carlo sign, and accurate calculations are feasible without using the extrapolation techniques developed to circumvent the “sign problem” [9].

The (isoscalar) surface-peaked interaction is assumed to be of the form  $v(\mathbf{r}, \mathbf{r}') = -\chi(dV/dr)(dV/dr')\delta(\hat{r} -$

$\hat{r}')$ , where  $V(r)$  is the mean-field potential. The angular delta function is expanded in multipoles, and only its quadrupole component is retained. Thus,

$$H_2 = - \sum_{\lambda\mu} \frac{\pi g_\lambda}{2\lambda + 1} P_{\lambda\mu}^\dagger P_{\lambda\mu} - \frac{1}{2} \chi : \sum_{\mu} (-)^\mu Q_\mu Q_{-\mu} :, \quad (1)$$

where  $::$  denotes normal ordering and  $P_{\lambda\mu}^\dagger, Q_\mu$  are pair and quadrupole operators given by

$$P_{\lambda\mu}^\dagger = \sum_{ab} (-)^\ell_b (j_a \parallel \mathcal{Y} \parallel j_b) [a_{j_a}^\dagger \times a_{j_b}^\dagger]_{\lambda\mu}, \quad (2)$$

$$Q_\mu = -\frac{1}{\sqrt{5}} \sum_{ac} \left( j_a \parallel \frac{dV}{dr} \mathcal{Y}_{2\mu} \parallel j_c \right) [a_{j_a}^\dagger \times \tilde{a}_{j_c}]_{2\mu}.$$

In (2)  $a \equiv n\ell j$  denotes a single particle orbit and  $\tilde{a}_{jm} = (-)^{j+m} a_{j-m}$ . The strength of the quadrupole interaction is determined by self-consistency. A change in the mean-field potential is related to a change in the one-body density  $\rho(\mathbf{r})$  through  $\delta V(\mathbf{r}) = \int d\mathbf{r}' v(\mathbf{r}, \mathbf{r}') \delta \rho(\mathbf{r}')$ . Using the invariance of the one-body potential under a displacement of the nucleus, and the separable form of the two-body interaction, we obtain

$$\chi^{-1} = \int_0^\infty dr r^2 \frac{dV}{dr} \frac{d\rho}{dr}. \quad (3)$$

The spherical nuclear density in (3) is calculated from  $\rho(r) = (4\pi)^{-1} \sum_a f_a R_a^2(r)/r^2$ , where  $f_a$  and  $R_a$  are the occupation number and the radial wave function of orbit  $a$ , respectively, and the sum goes over both the core and valence shells. In general we find that  $\chi \propto A^{-1/3}$  [6]. For  $^{124}\text{Xe}$ , Eq. (3) gives  $\chi = 0.018 \text{ MeV}^{-1} \text{ fm}^2$ , but this value must be renormalized since the interaction (1) is taken only in the valence shell. We find that a renormalization factor of  $\sim 3$  is required to reproduce correctly the variation of the excitation energy of the first

$2^+$  state in this region. We note that the value of the renormalization factor is expected to be larger than the standard value of 2 [10] since there are  $\Delta N = 0$  matrix elements that are not included in the model space, in addition to the usual  $\Delta N = 2$  elements [11].

The single-particle energies are determined from a Woods-Saxon plus spin-orbit potential using the parametrization of Ref. [12]. For  $^{124}\text{Xe}$ , the resulting single-particle energies of  $0g_{7/2}$ ,  $1d_{5/2}$ ,  $0h_{11/2}$ ,  $2s_{1/2}$ , and  $1d_{3/2}$  are  $-3.05$ ,  $-3.35$ ,  $-1.07$ ,  $-1.04$ , and  $-0.615$  MeV for protons and  $-11.79$ ,  $-12.08$ ,  $-9.53$ ,  $-10.21$ , and  $-9.94$  MeV for neutrons. The Coulomb potential has the effect of placing the  $h_{11/2}$  proton orbit below the  $d_{3/2}$  and  $s_{1/2}$  orbits. When the central Woods-Saxon potential is used for  $V(r)$  in (2), we find that the corresponding matrix elements of the quadrupole interaction in the proton single-particle basis differ by only a few percent from those in the neutron single-particle basis. We can therefore choose either set.

For the pairing interaction we include only monopole ( $\lambda = 0$ ) and quadrupole ( $\lambda = 2$ ) terms with  $g_0 = g_2$ . To determine  $g_0$  we first extract the pairing gap  $\Delta$  from the experimental masses of neighboring nuclei [13]. We then use a particle-projected BCS calculation for the Hamiltonian (1) to find the value of  $g_0$  that will reproduce the experimental gap for a spherical nucleus with the same mass number  $A$ . For  $^{124}\text{Xe}$  we find  $g_0 = 0.15$  MeV. The inclusion of quadrupole pairing is important in order to lower the excitation energy of the  $2_1^+$  state in the tin isotopes to about 1.3 MeV (which is  $2\Delta \sim 2$  MeV when only monopole pairing is included). Since both the monopole pairing and the quadrupole-quadrupole interaction are attractive, they satisfy the sign rule in the density decomposition and have a good Monte Carlo sign. The quadrupole pairing has components that violate the sign rule, but they are all very small in comparison with the good sign components. Setting all the bad components to zero has no more than a 5% effect on the spectrum. In identifying the bad components of the interaction, one should use the modified sign rule [9] since orbits of both parities are present in the 50–82 shell.

We begin discussion of our results with the probability distribution of the quadrupole moment  $Q_\mu \equiv \sum r^2 Y_{2\mu}$ . This probability distribution is defined as  $P(\mathbf{q}) \equiv \langle \prod_\mu \delta(Q_\mu - q_\mu) \rangle$  (where  $\mathbf{q} = \{q_\mu\}$ ) and is non-vanishing for  $\mathbf{q} \neq 0$  even if the ground state has  $J = 0$  and thus  $\langle Q_\mu \rangle = 0$ . The expectation value of an observable  $\Omega$  in the SMMC is calculated by a weighted integration over its values for noninteracting nucleons moving in a fluctuating auxiliary field:  $\langle \Omega \rangle_\sigma \equiv \text{Tr}(\Omega U_\sigma) / \text{Tr}(U_\sigma)$ , where the single-particle evolution operator associated with an auxiliary field  $\sigma$  is  $U_\sigma$ . In particular,  $P(\mathbf{q}) \propto \sum_\sigma \langle \prod_\mu \delta(Q_\mu - q_\mu) \rangle_\sigma$ , but this is difficult to calculate since it requires all moments  $\langle Q_\mu^n \rangle_\sigma$ . The method used in a recent SMMC study of deformed nuclei [5] follows

the prescription  $P(\mathbf{q}) \propto \sum_\sigma \prod_\mu \delta(\langle Q_\mu \rangle_\sigma - q_\mu)$ , which is valid provided  $\langle Q_\mu^n \rangle_\sigma = \langle Q_\mu \rangle_\sigma^n$ . We improve upon this prescription by explicitly forcing the quadratic moment to be correct. To that end, we calculate  $(\Delta_\sigma^2)_{\mu\nu} = \langle Q_\mu Q_\nu \rangle_\sigma - \langle Q_\mu \rangle_\sigma \langle Q_\nu \rangle_\sigma$  for each sample and assume that higher cumulants vanish. Then (in matrix notation)

$$P(\mathbf{q}) \propto \sum_\sigma \frac{1}{\det \Delta_\sigma} \exp \left[ -\frac{1}{2} (\langle \mathbf{Q} \rangle_\sigma - \mathbf{q})^T \times \frac{1}{\Delta_\sigma^2} (\langle \mathbf{Q} \rangle_\sigma - \mathbf{q}) \right]. \quad (4)$$

In order for (4) to define a shape distribution, we must associate a deformation  $\alpha_{2\mu}$  with each quadrupole moment  $\langle Q_\mu \rangle_\sigma$ . Starting from a deformed nucleus,  $R = R_0(1 + \sum_\mu \alpha_\mu Y_{2\mu}^*)$ , we calculate its quadrupole moment by expanding its density  $\rho(\mathbf{r}) \equiv \rho_0(r - R)$  (where  $\rho_0$  is the spherical density) to first order in deformation. We then find

$$\langle Q_\mu \rangle_\sigma = 4R_0 \left( \int_0^\infty r^3 \rho_0(r) dr \right) \alpha_{2\mu}, \quad (5)$$

where  $\rho_0$  is calculated as below Eq. (3), but only within the valence shell. The  $\alpha_{2\mu}$  are then transformed by rotation to the intrinsic frame where  $\alpha_{20} = \beta \cos \gamma$  and  $\alpha_{22} = \alpha_{2-2} = \beta \sin \gamma / \sqrt{2}$ , and (4) is used in the intrinsic frame to find  $P(\beta, \gamma)$ .

Typical shapes and their standard deviation are shown in the inset of Fig. 1. Rather than showing directly the shape distribution  $P(\beta, \gamma)$ , we convert it to a free energy surface through  $F(\beta, \gamma; T) \equiv -T \ln [P(\beta, \gamma) / \beta^3 |\sin 3\gamma|]$ , where the unitary metric  $\prod_\mu d\alpha_{2\mu} = \beta^4 |\sin 3\gamma| d\beta d\gamma d\Omega$  has been assumed [14]. Such free energy surfaces are shown in Fig. 1 for  $^{128}\text{Te}$  and  $^{124}\text{Xe}$  at different temperatures. These nuclei are clearly  $\gamma$ -soft, with energy minima at  $\beta_0 \sim 0.06$  and  $\beta_0 \sim 0.15$ , respectively. Energy surfaces calculated with Strutinsky-BCS using deformed Woods-Saxon potential [15] also indicates  $\gamma$ -softness with values of  $\beta_0$  comparable to the SMMC values. These calculations predict for  $^{124}\text{Xe}$  a prolate minimum with  $\beta_0 \approx 0.20$  which is lower than the spherical configuration by 1.7 MeV, but is only 0.3 MeV below the oblate saddle point, and for  $^{128}\text{Te}$  a shallow oblate minimum with  $\beta_0 \approx 0.03$ . These  $\gamma$ -soft surfaces are similar to those obtained in the O(6) symmetry of the IBM, or more generally, in cases where the Hamiltonian has mixed U(5) and O(6) symmetries but a common O(5) symmetry. In the Bohr Hamiltonian, an O(5) symmetry occurs when the collective potential energy depends only on  $\beta$  [1]. Our results are consistent with a potential energy  $V(\beta)$  that has a quartic anharmonicity [2] but a negative quadratic term that leads to a minimum at finite  $\beta_0$ .

We have also estimated total  $E2$  strengths from  $\langle Q^2 \rangle$  where  $Q = e_p Q_p + e_n Q_n$  is the electric quadrupole operator with effective charges of  $e_p = 1.5e$  and  $e_n = 0.7e$ , and extracted  $B(E2; 0 \rightarrow 2_1^+)$ , assuming that most

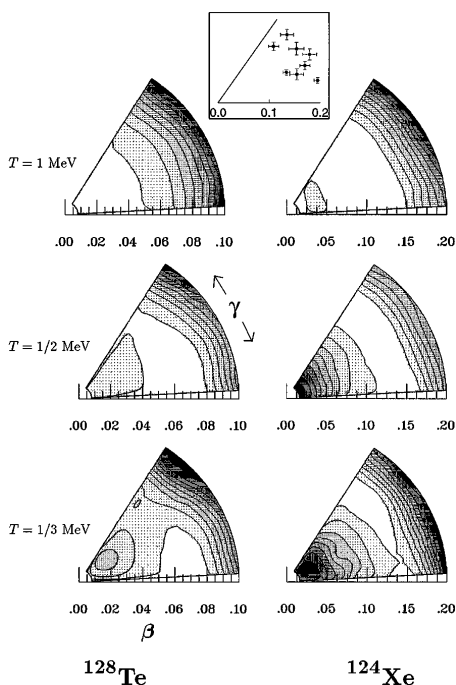


FIG. 1. Free energy surfaces for  $^{128}\text{Te}$  and  $^{124}\text{Xe}$  in the  $\beta$ - $\gamma$  plane at several temperatures. The contour lines are separated by 0.3 MeV and the lighter shades correspond to lower energies. Notice the  $\gamma$  softness of the surfaces. The surfaces are deduced from microscopically calculated shape distributions (see text). The inset illustrates a few typical shapes sampled in the SMMC and their standard deviation (for  $^{124}\text{Xe}$  at  $T = 1/3$  MeV).

of the strength is in the  $2_1^+$  state. We find  $B(E2; 0 \rightarrow 2_1^+)$  values of  $1314 \pm 10$ ,  $2856 \pm 15$ , and  $7248 \pm 36 e^2 \text{fm}^4$  to be compared with the experimental values [16] of 1660, 3830, and  $14900 e^2 \text{fm}^4$  for  $^{124}\text{Sn}$ ,  $^{128}\text{Te}$ , and  $^{124}\text{Xe}$ , respectively. The effective charges used are the theoretical estimates of [11] and are larger than their standard values because of a low-lying  $0\hbar\omega$  peak in the isoscalar strength function which is outside our model space. The SMMC calculations reproduce the qualitative trend; the quantitative discrepancy would be reduced had we used a renormalization factor similar to the potential field renormalization discussed above. A better quantitative agreement might be achieved by including additional subshells [17] and an isovector quadrupole interaction.

Information on excited states in SMMC can be obtained from strength functions. The energy centroid is given by  $\bar{E} = S_1/S_0$ , where  $S_n$  is the  $n$ th moment of the relevant strength function, and can be calculated from the first logarithmic derivative of the imaginary time response function. We calculated the  $2_1^+$  excitation energy this way from the  $E2$  response function. The values found of  $1.12 \pm 0.02$ ,  $0.96 \pm 0.02$ , and  $0.52 \pm 0.01$  MeV should be compared with the experimental values of 1.131, 0.743,

and 0.354 MeV for  $^{124}\text{Sn}$ ,  $^{128}\text{Te}$ , and  $^{124}\text{Xe}$ , respectively. The discrepancy for  $^{128}\text{Te}$  and  $^{124}\text{Xe}$  is due to contributions from the excited states at the finite temperature used in the calculations ( $T = 0.2$  MeV).

Another signature of softness is the response of the nucleus to rotations. We add a cranking field  $\omega J_z$  to the Hamiltonian and examine the moment of inertia as a function of the cranking frequency  $\omega$ . For a soft nucleus we expect a behavior intermediate between a deformed nucleus, where the inertia is independent of the cranking frequency, and the harmonic oscillator, where the inertia becomes singular. This is confirmed in Fig. 2 which shows the moment of inertia  $I_2 = d\langle J_z \rangle / d\omega = (\langle J_z^2 \rangle - \langle J_z \rangle^2) / T$  for  $^{124}\text{Xe}$  and  $^{128}\text{Te}$  as a function of  $\omega$ , and indicates that  $^{128}\text{Te}$  has a more harmonic character. The moment of inertia for  $\omega = 0$  in both nuclei is significantly lower than the rigid body value ( $\approx 43 \hbar^2/\text{MeV}$  for  $A = 124$ ) as a result of pairing correlations.

Also shown in Fig. 2 are  $\langle Q^2 \rangle$  where  $Q$  is the mass quadrupole, the BCS-like pairing correlation  $\langle \Delta^\dagger \Delta \rangle$  for the protons, and  $\langle J_z \rangle$ . Notice that the increase in  $I_2$  as a function of  $\omega$  is strongly correlated with the rapid decrease of pairing correlations, and that the peaks in  $I_2$  are associated with the onset of a decrease in collectivity (as measured by  $\langle Q^2 \rangle$ ). This suggests band crossing along the yrast line associated with pair breaking and alignment of the quasiparticle spins at  $\omega \approx 0.2$  MeV ( $\langle J_z \rangle \approx 7\hbar$ ) for  $^{128}\text{Te}$  and  $\omega \approx 0.3$  MeV ( $\langle J_z \rangle \approx 11\hbar$ ) for  $^{124}\text{Xe}$ . Our results are consistent with experimental evidence of band crossing in the yrast sequence of  $^{124}\text{Xe}$  around a spin

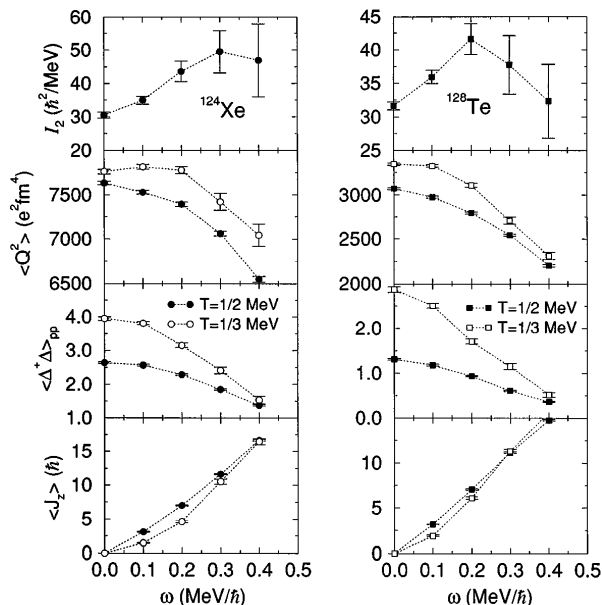


FIG. 2. Observables for  $^{124}\text{Xe}$  and  $^{128}\text{Te}$  as a function of cranking frequency  $\omega$  and for two temperatures.  $I_2$  is the moment of inertia,  $Q$  is the mass quadrupole moment,  $\Delta$  is the  $J = 0$  pairing operator, and  $J_z$  is the angular momentum along the cranking axis.

of  $10\hbar$  [18]. The alignment effect is clearly seen in the behavior of  $\langle J_z \rangle$  at the lower temperature, which shows a rapid increase after an initial moderate change. Deformation and pairing decrease as a function of both temperature and  $\omega$ .

We have analyzed the number of correlated pairs of these nuclei in their ground state. For a given angular momentum  $J$ , we define the pair operators  $A_{JM}^\dagger(ab) = 1/\sqrt{1 + \delta_{ab}} [a_{j_a}^\dagger \times a_{j_b}^\dagger]_{JM}$ . These operators are boson-like in the sense that they satisfy the expected commutation relations in the limit where the number of valence nucleons is small compared with the total number of single-particle states in the shell. In the SMMC we compute the pair correlation matrix in the ground state  $\sum_M \langle A_{JM}^\dagger(ab) A_{JM}(cd) \rangle$ , which is a Hermitian and positive-definite matrix in the space of ordered orbital pairs  $(ab)$  (with  $a \leq b$ ). This matrix can be diagonalized to find the eigenbosons  $B_{\alpha JM}^\dagger = \sum_{ab} \psi_{\alpha J}(ab) A_{JM}^\dagger(ab)$ , where  $\alpha$  labels the various bosons with the same angular momentum  $J$ . These eigenbosons satisfy

$$\sum_M \langle B_{\alpha JM}^\dagger B_{\gamma JM} \rangle = n_{\alpha J} \delta_{\alpha\gamma}, \quad (6)$$

where the positive eigenvalues  $n_{\alpha J}$  are the number of  $J$  pairs of type  $\alpha$ . We have calculated  $n_{\alpha J}$  in the various pairing channels for  $^{124}\text{Xe}$ . Since the number of neutrons in  $^{124}\text{Xe}$  is above 66, neutrons are treated as holes. For  $J = 0$  and  $J = 2$ , we can compare the largest  $n_{\alpha J}$  with the number of  $s$  and  $d$  bosons obtained from the O(6) limit of the IBM. In the latter we use the exact O(6) formula [3] for the average number of pairs and multiply by the relative fraction of protons and neutrons to find the pair content for each type of nucleon. For  $^{124}\text{Xe}$  the SMMC (IBM) results in the proton-proton pairing channel are 0.85 (1.22)  $s$  ( $J = 0$ ) pairs, and 0.76 (0.78)  $d$  ( $J = 2$ ) pairs, while in the neutron-neutron channel we find 1.76 (3.67)  $s$  pairs and 2.14 (2.33)  $d$  pairs. For the protons the SMMC  $d$  to  $s$  pair ratio 0.89 is close to its O(6) value of 0.64. However, this ratio for the neutrons, 1.21, is intermediate between its O(6) value of 0.64 and its SU(3) value of 1.64, and is consistent with the neutrons filling the middle of the shell. The total numbers of  $s$  and  $d$  pairs—1.61 proton pairs and 3.8 neutron (hole) pairs—are below the IBM values of 2 and 6, respectively. Our fermion-based SMMC calculations thus indicate pair correlations for  $J > 2$ .

In conclusion, we have presented the first microscopic evidence of softness in nuclei in the 100–140 mass

region, using the SMMC for the full 50–82 major shell. Future work will include an isovector quadrupole force. However, such calculations are more time consuming as this interaction violates the Monte Carlo sign rule.

This work was supported in part by the U.S. Department of Energy, Contracts No. DE-FG-0291-ER-40608, No. DE-FG0690-ER40561, and No. DE-AC05-96OR22464, and by the National Science Foundation, Grants No. PHY90-13248 and No. PHY91-15574. Computational cycles were provided on the IBM SP2 at the Maui High Performance Computing Center. We acknowledge useful discussions with F. Iachello, H. Nakada, and A. Ansari. Y. A. acknowledges the hospitality of the Institute for Nuclear Theory at the University of Washington where part of this work was completed.

- 
- [1] L. Willets and M. Jean, *Phys. Rev.* **102**, 788 (1956).
  - [2] O. Vorov and Zelevinsky, *Nucl. Phys.* **A439**, 207 (1985).
  - [3] F. Iachello and A. Arima, *The Interacting Boson Model* (Cambridge Univ. Press, Cambridge, U.K., 1987); W. Krips *et al.*, *Nucl. Phys.* **A529**, 485 (1991); T. Otsuka, *Nucl. Phys.* **A557**, 531c (1993).
  - [4] G.H. Lang, C.W. Johnson, S.E. Koonin, and W.E. Ormand, *Phys. Rev. C* **48**, 1518 (1993).
  - [5] D.J. Dean, S.E. Koonin, G.H. Lang, P.B. Radha, and W.E. Ormand, *Phys. Lett. B* **317**, 275 (1993).
  - [6] M. Dufour and A. Zuker, LANL archives Report No. nucl-th/9505010.
  - [7] R. Broglia, D.R. Bes, and B.S. Nilsson, *Phys. Lett.* **50B**, 213 (1974).
  - [8] B. Lauritzen and G.F. Bertsch, *Phys. Rev. C* **39**, 2412 (1989).
  - [9] Y. Alhassid, D.J. Dean, S.E. Koonin, G. Lang, and W.E. Ormand, *Phys. Rev. Lett.* **72**, 613 (1994).
  - [10] D.R. Bes and R.A. Sorenson, *Adv. Nucl. Phys.* **2**, 129 (1969).
  - [11] H. Sagawa, O. Scholten, B.A. Brown, and B.H. Wildenthal, *Nucl. Phys.* **A462**, 1 (1987).
  - [12] W. Nazarewicz, J. Dudek, R. Bengtsson, T. Bengtsson, and I. Ragnarsson, *Nucl. Phys.* **A435**, 397 (1985).
  - [13] A. Bohr and B. Mottelson, *Nuclear Structure* (Benjamin, New York, 1969), Vol. I.
  - [14] Y. Alhassid and B. Bush, *Nucl. Phys.* **A509**, 461 (1990).
  - [15] R. Wyss and W. Nazarewicz (private communication).
  - [16] S. Raman *et al.*, *Atomic Data Nucl. Data Tables* **36**, 1 (1987).
  - [17] A.P. Zuker, J. Retamosa, A. Poves, and E. Caurier, *Phys. Rev. C* **52**, R1741 (1995).
  - [18] W. Gast *et al.*, *Z. Phys. A* **318**, 123 (1984).